Segmentation of Thoracic Computed Tomography Images

Sébastien VAUCLIN [1], Peng ZHANG [1,2], Isabelle GARDIN [1,3],
Olivier GALLOCHER [4], Patrick VANNOORENBERGHE [2]

[1] Laboratoire Universitaire Quantification en Imagerie Fonctionnelle
Université de Rouen, Faculté de Médecine, 76000 ROUEN, France
[2]Laboratoire Perception Systèmes Information, FRE 2645 CNRS
Université de Rouen, Place Emile Blondel, 76821 MONT SAINT AIGNAN CEDEX, France
[3] Département de Médecine Nucléaire, CHB-CHU, 76000 ROUEN, France
[4] Département de Radiothérapie et Physique Médicale, CHB, 76000 ROUEN, France

***Abstract*— Segmentation of thoracic computed tomography (CT) images is an important step in many medical imaging applications. This paper presents an automatic scheme for identifying the patient's contour, the lungs, the trachea and the spinal canal on a set of two-dimensional (2D) thoracic CT images. Three different methods were proposed for the segmentation process. An adaptive thresholding method was used for the delineation of the external skin surface of the patient. A 3D credal filter, based on the belief functions theory, was implemented for the lungs and the spinal canal segmentation. Because of the differences between the organs shape, the filter parameters were different. For the lung, no direction was privileged, whereas for the spinal canal the perpendicular direction of the transverse slices was privileged in order to reinforce the inter-slice contribution. A 3D region growing method was used for the trachea segmentation. Segmentation results on a set of 2D CT images are presented and allows to highlight the performances of the proposed methodology. The contours were evaluated by an experimented radiation oncologist.**

I. Introduction

The identification and delineation of organs at risk (lung, spinal cord, oesophagus, heart) are essential steps in the planning of radiation treatment for lung cancer. The regions occupied by these structures must be defined accurately to ensure that therapeutic goals are satisfied. Modern treatment planning systems (TPSs) allow users to draw contours around regions of interest based on transverse computed tomography images. Several semi automatic tools have been developed contouring the patient's body, the lung and the spinal cord, but with a manual adjustment. For the other organs, this process is largely carried out by hand. It is time-consuming and subject to user variability. Most of CT images segmentation relies on thresholding of CT Hounsfiels units (HU) using fixed or chosen threshold values. This approach gives relatively good results for those structures that are completely enclosed by tissues with HU values significantly different from their own. For structures that are only partially surrounded by tissues with significantly different HU values, thresholding techniques often fail.

Several authors have developed tools for computer assisted segmentation of medical images. Hu et al. [1] proposed a completely 2D automatic method for lung segmentation on CT images using an adaptive thresholding technique. Hedlund et al. [2] also presented two methods for lung segmentation. The first one is based on finding the steep density gradient between low density of lung (HU less than -600 HU) and high density of chest wall (HU higher than -550 HU), by an edge tracking method. The principle of the second method is to select all voxels contiguous (i.e. supposed as lung voxels) with a single starting point in the lung that are also within a specified HU range and have an average difference of less than a specified value. Kiraly and al. [3] proposed two algorithms for the trachea segmentation on CT images: i) an adptative region-growing method and ii) a hybrid algorithm that uses both region growing and mathematical morphology. The aim was to obtain a virtual bronchoscopy. More recently, the evidence theory [4], [5], [6], [7] was used for brain tissues segmentation on Magnetic Resonance Imaging (MRI) [8], [9], [10], [11], but not on pulmonary CT imaging to our knowledge.

In this paper, we describe an automatic scheme for identifying the contour of the patient's body, the right and left lungs, the trachea and the spinal canal on pulmonary CT images for external radiotherapy purpose. The proposed methodology is based on three main algorithms to segment such a variety of organs shapes. Firstly, to define the body contour, an adaptative thresholding followed by a morphological opening method was used (section II-A). Secondly, inside this volume of interest, i) a 3D credal filter, based on the belief functions theory, (section II-B) was applied for lungs and spinal canal segmentation, ii) a 3D region growing algorithm (section II-C) was used for the trachea segmentation. Segmentation results are presented on 2D thoracic CT images to highlight the performance of this methodology (section III).

II. Material and Methods

A. Patient's contour delineation

The goal of this step is to determine the external skin surface. The obtained volume of interest makes it possible to decrease largely the execution time while increasing the segmentation precision. All "useless" information is isolated for future calculation. Rather than using a fixed threshold value to define the body contour, we used the adaptive thresholding method proposed by Hu et al. [1]. Morphological operations were then applied for improving the body contour definition.

1) Adaptive thresholding: The segmentation threshold is selected through an iterative procedure. Let T^i be the segmentation threshold at step i. To choose a new segmentation threshold, T^i is applied to the image to separate high density (HD) voxels (soft tissues and bone structures) from low density (LD) voxels (lungs, trachea and air surrounding the body). Let μ_h and μ_l be the mean gray-level of HD voxels and LD voxels after segmentation with threshold T^i. Then the new threshold for step $i+1$ is obtained using:

$$T^{i+1} = \frac{\mu_h + \mu_l}{2}. \tag{1}$$

This iterative threshold update procedure is repeated until there is no change in the threshold, i.e., $T^{i+1} = T^i$.

2) Morphological operations: During the previous step, some voxels that don't belong to the patient are labeled as HD, for instance, the examination table where the patient is lying during the CT acquisition. On transverse slices, the table corresponds to a very fine structure. It was removed by a set of 8 "opening" morphological operations [12] with a circle as filter of radius 1 pixel.

B. Segmentation of lungs and spinal canal

In this step, the 3D credal filter, based on the belief functions theory (BFT) [4], was performed for lungs and spinal canal segmentation. BFT provides an interesting framework to aggregate evidence of multiple information sources (i.e. neighborhood voxels). BFT deals with uncertainty and imprecision in three levels: i) representing evidence by focal elements and masses, ii) combining evidence by the Dempster's rule, and iii) making decisions.

Firstly, a K-means clustering algorithm [13] is used in order to performed a pre-segmentation. Then a 3D filter exploits the results of the pre-segmentation to compute the membership degree from spatial neighbors using belief functions [5], [6]. Formally, the segmentation of a volumic image $\mathcal{I}$ defined on a set of voxels $\mathcal{V} = \{V_1, \ldots, V_N\}$ is a partition of $\mathcal{V}$ in non-empty disjoint subsets $\mathcal{R}_k$ for $k = 1, 2, \cdots, K$ called regions containing connected voxels. The partition $\mathcal{V}$ verifies $\mathcal{V} = \bigcup_{k=1}^{K} \mathcal{R}_k$.

The segmentation principle consists in clustering CT data viewed as voxels in the volumic images. A region $\mathcal{R}_k$ is considered as a set of connected voxels belonging to the same class ω_k in the frame of discernment Ω which is defined as a finite set of hypotheses ω_k for $k = 1, 2, \cdots, K$. In order to quantify the membership degree for each voxel in the volume, the frame of discernment Ω was defined by a semi-supervised methodology. The number of classes (i.e. 3D regions) is manually adjusted by the user while the clusters parameters are extracted using a K-means clustering algorithm [13]. Each class $\omega_k \in \Omega$ can be represented by its center of gravity C_k defined as:

$$C_k = C(\omega_k) = \frac{1}{|\omega_k|} \sum_{i=1}^{|\omega_k|} x_i \tag{2}$$

where x_i is the Hounsfield units of voxel V_i. In this equation, $|\omega_k|$ represents the cardinality (number of voxels) of class ω_k after the clustering algorithm. This K-means clustering algorithm obtain unsatisfactory results because it does not take into account the spatial information contained in CT images. Thus, a credal filter is applied in order to improve the segmentation results.

Details of 3D credal filter are given in case of voxel V with its corresponding neighbors $\Phi(V)$[1]. According to Ω, a basic belief assignment (bba) m_i is first built for each voxel V_i belonging to the neighbors of the studied voxel V ($V_i \in \Phi(V)$). This function quantifies the degree of belief concerning the membership of the voxel V to a class (region) in Ω. Each bba m_i is thus related to the frame of discernment Ω previously defined with K-means algorithm. We chose to compute bba m_i associated to voxel V_i following the relationships:

$$m_i(\{\omega_k\}) = \alpha_i^{'} \exp[-\gamma(d_{i,k})] \tag{3}$$

$$m_i(\Omega) = 1 - \alpha_i^{'} \exp[-\gamma(d_{i,k})] \tag{4}$$

where $d_{i,k}$ is the Euclidean distance between the gray level of voxel V_i and class center C_k. The degree of belief allocated to singleton ω_k is just an $\alpha_i^{'}$-attenuation of the distance between the gray level of the studied voxel V_i and center of the class ω_k. The value of $\alpha_i^{'}$ can be computed using:

$$\alpha_i^{'} = \alpha_i . \beta \tag{5}$$

where α_i is selected in [0,1] and adjusted according to the distance between the voxel V_i and voxel V we want to classify (i.e., more the source is near and more it will be reliable). β is an attenuation coefficient which takes into account the inter-slice distance information. For each voxel V, bba's corresponding to each neighbor are then aggregated to obtain an unique bba $m_\oplus$ defined on Ω using Dempster's rule of combination [4]. This function can be computed using:

$$m_\oplus = \bigoplus_{V_i \in \Phi(V)} m_i. \tag{6}$$

The fusion of all voxels V_i located in the neighborhood of V allows to take into account the weighted opinions on the membership of the voxel V in Ω. Finally, the decision to

[1]Application of a 3D filter for a voxel V takes into account information resulting from its 26 neighbors: filter size 3×3 for slice $n-1$ (9 neighbors), n (8 neighbors), $n+1$ (9 neighbors)

assign the voxel V to a class in Ω is taken while analyzing the pignistic probability [7] obtained using equation:

$$BetP(\omega_k) = \sum_{A \subseteq \Omega, \omega_k \in A} \frac{m_{\oplus}(A)}{|A|.(1 - m_{\oplus}(\emptyset))} \quad (7)$$

where $|A|$ is the cardinality of A. The maximum value of $BetP$ is taken for decision making.

C. Trachea segmentation

A 3D region growing algorithm [3] was chosen and implemented for segmentation of the trachea. Firstly, a seed point belonging to the trachea is manually selected. The initial segmented region consists in this single voxel. The region is then iteratively expanded by checking if any adjacent voxels to the region satisfy a connectivity criteria [2]. When the process stops to include new voxels, the result is a contiguous region of connected voxels that all satisfy the pre-defined criteria. We decided to use a 6-connected region[3]. In this way, the algorithm progressively fills the trachea, including more and more voxels, and finally include the entire trachea.

III. Results and discussion

The performances of our methodology were evaluated on thoracic computed tomography images and illustrated on one patient. The acquisition of the entire thorax was performed under free breathing, in treatment position without any intraveinous contrast administration. The 3D pulmonary volume corresponded to a stack of 64 contiguous 2-D transverse slices of 512×512 voxels (slice thickness: 5 mm and voxel size: 0.75 mm). The contours were evaluated by an experimented radiation oncologist. The results are presented in case of three different slices (Fig. 1 top). The first one (a) is located at the superior level of lung (under the clavicles), the second one (b) at the median part of lungs (at the level of the tracheal bifurcation), while the third one (c) is under the diaphragm.

A. Patient's contour delineation

The patient's contour definition was carried out using the adaptative thresholding algorithm followed by the morphological opening method. The first threshold value T^0 was arbitrary selected to 0. The number of iterations was 56, and the final μ_h and μ_l values were -8.68 HU and -973.32 HU respectively. The corresponding contour is presented Fig. 1 for the 3 slices (bottom). The analysis of segmented images shows the good performances of the implemented method. We can note:

- The good delineation of the external skin surface by using an arbitrary first threshold value which was very different from the final threshold value (i.e. 0 HU vs -473 HU).
- The examination table, on which the patient was lying, was almost completely removed except on some slices, in spite of the fact that it has a HU value of the same order of magnitude as that of soft tissues.

[2]The simplest connectivity criteria is simply to accept very dark regions, i.e. growing when the level was below than a threshold level T.

[3]Voxels could be connected in 6 directions: up, down, north, east, south, west.

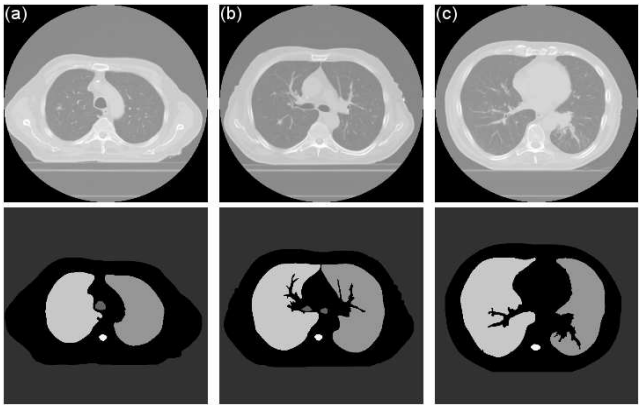

Fig. 1. CT thoracic image segmentation of body, lungs and trachea: (a) Slice 17, (b) Slice 27, (c) Slice 39.

B. Lungs and spinal canal segmentation

For lung and spinal canal segmentation, the 3D credal filter was used. For the lungs, the filter was applied on the volume of interest defined during the patient's contour definition (darkest regions on images of Figure 1). Whereas, it was applied on a cubic volume, including the spinal column for the spinal canal segmentation. Each time, the voxels classification concerned 2 classes, the volume of interest (i.e. the lung or the spinal canal) and the other anatomical structures. Because of the differences between the two organs shape, the 3D credal filter parameters were different. For the lungs, there is no privileged direction, whereas for the spinal canal the main direction is perpendicular to the transverse 2D-slices. Thus, the inter-slices contribution must be promoted. The following parameters for 3D credal filter were used in case of lungs segmentation: $\alpha_i^{'} = 0.9$ for slice n, $\alpha_i^{'} = 0.135$ for slices $n-1$ and $n+1$, $\gamma = 0.05$, filter size = 3×3 and $\Omega = \{-850, -550\}$. With these adjustments, slices $n-1$ and $n+1$ are discounted and have a weak contribution concerning the decision made for slice n. Mean values for the classes centers are obtained using the K-means algorithm as explained in section II-B. The

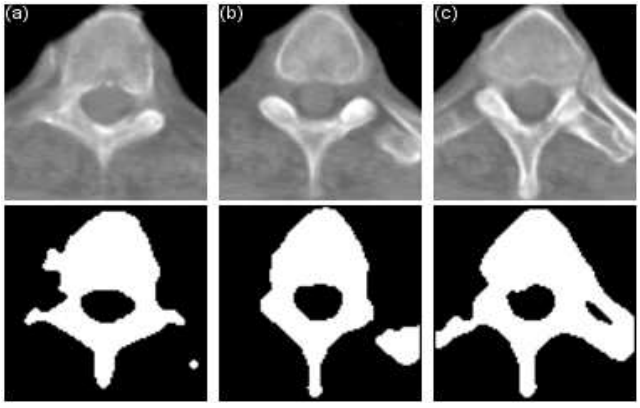

Fig. 2. CT thoracic image segmentation of spinal canal: (a) Slice 10. (b) Slice 11. (c) Slice 12.

segmentation results are given Fig. 1 for the 3 slices (bottom).

On the other hand, for spinal canal segmentation, parameters are following: $\alpha_i^{'} = 0.9$ for slice n, $\alpha_i^{'} = 0.72$ for slices $n-1$ and $n+1$, $\gamma = 0.05$, filter size = 5×5 and $\Omega = \{50, 80\}$. To illustrate the influence of the high contribution of slices $n-1$ and $n+1$ on the spinal canal segmentation of slice n, an example of three consecutive CT slices are given on top of Fig. 2. The corresponding segmentation is given on the bottom of the same figure. It's obvious that the bone structures surrounding the spinal canal are very different on the CT slices. Bone structure doesn't surround the spinal canal completely, whereas on segmented slices, the spinal canal region is totally surrounded by what we can call a "reconstructed bone structure".

From the segmented images analysis, we can note the good performances of the implemented method showing its ability to modulate the 3D information coming from the neighborhood voxels as well as the neighborhood slices ($n-1$ and $n+1$). The credal filter permits to reduce connection risks between trachea and lung when they are very close, and between the left and right lungs at the anterior or posterior junctions (see an example slice (b) on Fig. 1). The method allows an accurate spinal canal segmentation.

C. Trachea segmentation

For the trachea segmentation, the 3D region growing algorithm was implemented. The seed point is first manually selected at the upper part of the trachea, since the size makes it easy to identify. The threshold value T was then selected to -270 HU. The number of iterations to treat 23 slices (from slice 1 to slice 23) was 12935. The bottom part of Fig. 1 illustrates the good performances of the algorithm, in particular, its ability to separate the right and left parts of the trachea under the tracheal bifurcation (see slice b). For this 3D region growing algorithm, future work concerns the automatic adjustment of the threshold. Integration of some morphological information concerning the anatomical structure to be segmented is also investigated.

IV. Conclusion

In this article, a semi-automatic segmentation scheme was proposed for identifying the patient's contour, the lungs, the spinal canal and the trachea on a set of two-dimensional (2D) thoracic CT images.

Because of the difference between organs shape, three different methods were proposed for the segmentation process. An adaptive thresholding method was used for the delineation of the external skin surface. A 3D credal filter, based on the belief functions theory, was implemented for the lungs and the spinal canal segmentation. Two sets of filter parameters were used. For the lung, no direction was privileged, whereas for the spinal canal the perpendicular direction of the transverse slices was privileged in order to reinforce the inter-slice contribution. Finally, a 3D region growing method was used for the trachea segmentation.

Future works are concerned with automatic adjustment of the 3D credal filter parameters according to the anatomical constraints associated to the volumes to be segmented. This can be done using additional knowledge given by the experts. The credal filter can be extended at continuous level (while considering continuum instead finite set of classes) using specific belief functions [14]. This is under investigation. Improvements must also be carried out for a complete elimination of the examination table during the patient's contour delineation. Another important issue is to validate the presented methodology using a series of patients according to specific criteria to be determine by radiation oncologists.

V. Acknowledgements

This work is supported by the regional council of 'Haute Normandie'.

Authors would like to cordially thank the Department of Radiotherapy and Medical Physics (CHB - Rouen) for their precious help.

References

[1] S. Hu, E.A. Hoffman, and J.M. Reinhardt, "Automatic lung segmentation for accurate quantitation of volumetric x-ray CT images," *IEEE Transactions on Medical Imaging*, vol. 20, no. 6, pp. 490–498, JUNE 2001.

[2] L.W. Hedlund, R.F. Anderson, P.L. Goulding, J.W. Beck, E.L. Effmann, and C.E. Putman, "Two methods for isolating the lung area of a ct scan for density information," *Radiology*, vol. 144, pp. 353–357, July 1982.

[3] A.P. Kiraly, W.E. Higgins, E.A. Hoffman, G. McLennan and R.M. Reinhardt, "3D human airway segmentation for virtual bronchoscopy," in *SPIE Medical Imaging*. 2002, vol. 4683, pp. 16–29, SPIE press.

[4] A. Dempster, "Upper and lower probabilities induced by multivalued mapping," *Annals of Mathematical Statistics*, vol. AMS-38, pp. 325–339, 1967.

[5] G. Shafer, *A Mathematical Theory of Evidence*, Princeton University Press, 1976.

[6] P. Smets, "Quantifying beliefs by belief functions: an axiomatic justification," in *Proceedings of the 13th International Joint Conference on Artificial Intelligence*, San Mateo, CA, 1993, pp. 598–603, Morgan Kaufmann.

[7] P. Smets and R. Kennes, "The transferable belief model," *Artificial Intelligence*, vol. 66, no. 2, pp. 191–234, 1994.

[8] A.-S. Capelle, C. Fernandez-Maloigne, and O. Colot, "Segmentation of brain tumors by evidence theory: On the use of the conflict information," in *Proceedings of the Seventh International Conference on Information Fusion*, Jun 2004, vol. I, pp. 264–271.

[9] I. Bloch, "Some aspects of Dempster-Shafer evidence theory for classification of multi-modality medical images taking partial volume effect into account," *Pattern recognition Letters*, vol. 17, pp. 905–919, 1996.

[10] H. Zhu and O. Basir, "Adaptive fuzzy evidential reasoning for automated brain tissue segmentation," in *Proceedings of the Seventh International Conference on Information Fusion*. Jun 2004, vol. I, pp. 272–279, International Society of Information Fusion.

[11] H. Zhu and O. Basir, "Extended discounting scheme for evidential reasoning as applied to MS lesion detection," in *Proceedings of the Seventh International Conference on Information Fusion*. Jun 2004, vol. I, pp. 280–287, International Society of Information Fusion.

[12] J. Serra, "Analysis and mathematical morphology," *Academic Press*, 1982.

[13] J.C. Bezdek, J. Keller, R. Krishnapuram, and N.R. Pal, *Fuzzy Models and Algorithms for Pattern Recognition and Image Processing*, Kluwer Academic Publishers, 1999.

[14] B. Ristic and Ph. Smets, "Belief function theory on the continuous space with an application to model based classification," in *International Conference IPMU'2004*, 2004, pp. 1119–1126.